NUMERICAL SIMULATION OF PARTICLE TRAJECTORIES IN INHOMOGENEOUS TURBULENCE, III: COMPARISON OF PREDICTIONS WITH EXPERIMENTAL DATA FOR THE ATMOSPHERIC SURFACE LAYER

J. D. WILSON*, G. W. THURTELL, and G. E. KIDD

Department of Land Resource Science, University of Guelph, Guelph, Ontario, Canada

(Received 31 December, 1980)

Abstract. It is shown that predictions of a numerical trajectory-simulation method agree closely with the Project Prairie Grass observations of the concentrations 100 m downwind of a continuous point source of sulphur dioxide if the height (z) dependence of the Lagrangian length scale Λ_L is chosen as:

$$\Lambda_L = 0.5z\left(1 - 6\frac{z}{L}\right)^{1/4} \qquad L < 0$$

$$\Lambda_L = 0.5z/\left(1 + 5\frac{z}{L}\right) \qquad L > 0$$

where L is the Monin–Obukhov length. The value of 0.5 for Λ_L/z in neutral conditions is consistent with the findings of Reid (1979) for the Porton experiment, and is also shown to be the best choice for simulation of an experiment in which concentration profiles were measured a short distance (< 40 m) downwind of an elevated point source of glass beads (40 μm diameter).

1. Introduction

Two previous papers (Wilson *et al.*, 1981a, b; hereafter referred to as I, II) have described a method of simulation of fluid element (or particle) trajectories in systems which have Eulerian velocity field (u, 0, w) relative to axes (x, y, z) and in which the Eulerian velocity, time and length scales of the turbulence, σ_w, τ, $\Lambda = \sigma_w\tau$, vary only in the z direction. The velocity u is a function of z alone, and the time average value of w is zero.

Vertical and horizontal steps are calculated using

$$\begin{aligned}
\Delta z &= \left[w_L(t_H) + \bar{w}_{*L} + \bar{w}_{g^*}\right]\frac{\sigma_w(z)}{\sigma_w(H)}\frac{\tau_L(z)}{\tau_L(H)}\Delta t_H \\
&= \frac{\Lambda_L(z)}{\Lambda_L(H)}\Delta z_* \\
\Delta z_* &= \left[w_L(t_H) + \bar{w}_{*L} + \bar{w}_{g^*}\right]\Delta t_H \qquad (1) \\
\Delta x &= u(z)\frac{\tau_L(z)}{\tau_L(H)}\Delta t_H.
\end{aligned}$$

* Present affiliation: New Zealand Meteorological Service, P.O. Box 722, Wellington, New Zealand.

Boundary Layer Meteorology **21** (1981) 443–463. 0006–8314/81/0214–0443$03.15.

The Lagrangian timescale $\tau_L(z)$ is defined by

$$\tau_L(z) = \int_0^\infty R_L(z, \xi)\, d\xi$$

where R_L is the Lagrangian autocorrelation function

$$R_L(z, \xi) = \overline{w_L(t|z(t_0))w_L(t + \xi|z(t_0))}^E / \overline{w_L^2(z(t_0))}^E.$$

The E denotes an ensemble average. $R_L(z, \xi)$ is defined with respect to an ensemble of experiments in each of which at time t_0 a marked fluid element is released at height z and thereafter followed. The variance

$$\overline{w_L^2}^E(z(t_0)) \equiv \sigma_L^2(z)$$

is formed from the velocities of the fluid elements at height z at the time of release. It is assumed that

$$\sigma_L(z) = \sigma_w(z)$$
$$\tau_L(z) \propto \tau(z)$$

so that

$$\Lambda_L(z) = \sigma_w(z)\tau_L(z) \propto \Lambda(z).$$

Particle trajectories are calculated in the transformed coordinates (x, z_*, t_H) in which the turbulence is homogeneous (constant length, time, and velocity scales). t_H is related to real time by

$$\frac{dt_H}{\tau_L(H)} = \frac{dt}{\tau_L(z)},$$

and the time step Δt_H is chosen as $\Delta t_H \simeq (\tau_H/10)$, where $\tau_H = \tau_L(H)$.

The fluctuating Lagrangian velocity $w_L(t_H)$ is a record of vertical velocity appropriate to particle movement at the 'reference height', H; in our work this is obtained by applying a single-stage low-pass RC filter to the output of a random noise generator (Hewlett-Packard, model 3722 A)*. An alternative method of generating $w_L(t_H)$ is the Markov chain

$$w_L(t_H + \Delta t_H) = w_L(t_H) \exp\left(-\frac{\Delta t_H}{\tau_H}\right) + \left[1 - \exp\left(\frac{-2\Delta t_H}{\tau_H}\right)\right]^{1/2} \sigma_w(H)\, r$$

where r is chosen at random from a normal distribution with mean zero and variance 1. Careful comparison showed there was no detectable difference between concentration profiles generated by these two choices for $w_L(t_H)$.

$\bar{w}_{*L}$ is a bias velocity, given by

$$\bar{w}_{*L} = \sigma_w(H)\tau_L(z)\frac{\partial \sigma_w}{\partial z}$$

* Hewlett-Packard, Palo Alto, California, 94304, U.S.A.

and has equivalent in the z system

$$\bar{w}_L = \Lambda_L(z)\frac{\partial \sigma_w}{\partial z}.$$

In a system with σ_w = constant, $\bar{w}_{*L}$ vanishes and

$$\frac{\Lambda_L(z)}{\Lambda_L(H)} = \frac{\tau_L(z)}{\tau_L(H)}.$$

The other velocity is the z_* equivalent of the real world gravitational settling velocity $\bar{w}_g$,

$$\bar{w}_{g^*} = \frac{\sigma_w(H)}{\sigma_w(z)}\bar{w}_g.$$

The z_* axis is divided into 200 layers of depth Δz_*, where the midpoint of each layer is given by $z_*(\mathrm{I}) = (\mathrm{I}-0.5)\Delta z_*$. Prior to calculation of a set of trajectories, the $z(\mathrm{I})$ corresponding to each $z_*(\mathrm{I})$ are calculated by integrating the relationship

$$\mathrm{d}z = \frac{\Lambda_L(z)}{\Lambda_L(H)}\mathrm{d}z_*.$$

Depending on the expression chosen for $\Lambda_L(z)$, this may be performed analytically or numerically. In the case of the expressions for $\Lambda_L(z)$ recommended as a result of this work, analytical integration yields a relationship between z and z_* which is implicit in z. This was solved to obtain the $z(\mathrm{I})$ using Newton's Method of Successive Approximations (Abramowitz and Stegun, 1970). Once the $z(\mathrm{I})$ are obtained, tables of

$$\Delta x(\mathrm{I}) = u(z(\mathrm{I}))\frac{\tau_L(z(\mathrm{I}))}{\tau_L(H)}\Delta t_H$$
$$\mathrm{WBAR(I)} = \bar{w}_{*L}(\mathrm{I}) + \bar{w}_{g^*}(\mathrm{I})$$

are defined. Each step of a trajectory is then calculated as

$$\Delta z_* = (w_L(t_H) + \mathrm{WBAR(I)})\,\Delta t_H$$
$$\Delta x = \Delta x(\mathrm{I})$$

where I is obtained from the instantaneous value of z_*.

It is the intention in this paper to compare concentration profiles obtained by performing ensemble experiments in which many trajectories are calculated using Equations (1) with concentration profiles measured in the atmospheric surface layer under neutral, unstable, and stable conditions. Two experiments will be discussed:

(i) Project Prairie Grass (Barad, 1958; Haugen, 1959) in which SO_2 was used as a tracer;

(ii) An experiment performed at the University of Guelph in which spherical glass beads, 40 μm in diameter, were used as a tracer.

Both experiments employed a point source with several detectors placed on a circular arc centred on the source. Let the wind field be (u_1, v_1, w_1). At any given radius and height, a lateral concentration profile is obtained whose lateral spread about the mean wind direction and peak height are related to the spectrum of the cross-wind component. By integration of this profile in the lateral direction, one may estimate the concentration which would be observed if the wind field was strictly two-dimensional, $(u, 0, w)$ with $u = \sqrt{u_1^2 + v_1^2}$, the 'cross-wind integrated concentration', or equivalent two-dimensional concentration. Note that u is the windspeed which is measured by a cup anemometer.

In order to apply Equations (1) to calculate trajectories in the surface layer, it is necessary to determine the behaviour of $\sigma_w(z)$ and $\tau_L(z)$. Measurements of σ_w (see Haugen, 1973) have determined that

$$\sigma_w \simeq 2u_*\left(\frac{z}{-L}\right)^{1/3} \quad \text{for} \quad \frac{z}{L} < -0.5$$

$$\sigma_w \simeq 1.25u_* \quad \text{for} \quad -0.5 < z/L$$

where

u_* = friction velocity = $(-\overline{uw})^{1/2}$

L = Monin–Obukhov length = $-u_*^3 \Big/ \left(k \frac{g}{T_0} \frac{H}{\rho c_p}\right)$

H = sensible heat flux = $\rho c_p \overline{w T}$

g = acceleration due to gravity

c_p = specific heat at constant pressure

ρ = density of the air

k = von Karman's constant (0.4 used herein)

T = temperature

T_0 = reference temperature.

The choice of $\sigma_w(z)$ used for trajectory simulation in the very unstable surface layer (under conditions where one might expect a large number of particles to travel to heights $z \gtrsim -L/2$) was

$$\sigma_w = \beta u_*\left(1 + 4.1\frac{z}{-L}\right)^{1/3}$$

with $\beta = 1.25$ unless a measurement of σ_w was available and implied the need for a different choice.

Under stable and slightly unstable stratification, we used

σ_w = constant
= measured value (if available)
= 1.25 u_* (otherwise).

Direct measurements of the Eulerian timescale $\tau(z)$ in the surface layer have not often been reported. Ward (1977) found $\sigma_w(z)\tau(z) = 0.1z$ in and above a corn canopy, by measuring σ_w and calculating $\tau(z)$ from the measured autocorrelation function. It is widely expected that $\tau(z)$ will be a linear function of z in neutral conditions for $z \gg z_0$, because σ_w = constant and eddy viscosity has been observed to increase linearly with z. A possible approach to determining τ_L for non-neutral stratification is to relate the stability dependence of the eddy diffusivity $K = \sigma_w^2 \tau_L$ of a passive additive to that of K_w, the diffusivity for water vapor, which is given by

$$K_w = ku_* z/\phi_w\left(\frac{z}{L}\right)$$

where ϕ_w is a universal function of z/L, defined by

$$\frac{kz}{q_*}\frac{\partial \bar{q}}{\partial z} = \phi_w\left(\frac{z}{L}\right).$$

Here $q_* = E/\rho u_*$; $E = \rho\,\overline{qw}$, the latent heat flux; q = specific humidity. Dyer and Hicks (1970) found

$$\phi_w = \left(1 - 16\frac{z}{L}\right)^{-1/2} \quad \text{for} \quad -1.0 \leq \frac{z}{L} < -0.01$$

and Webb (1970) found

$$\phi_w = \left(1 + 5.2\frac{z}{L}\right) \quad \text{for} \quad 0 < \frac{z}{L}.$$

Therefore if we can regard water vapour as a passive additive,

$$K = K_w = ku_* z\left(1 - 16\frac{z}{L}\right)^{1/2} \quad \text{(unstable)}$$

$$K = K_w = ku_* z/\left(1 + 5.2\frac{z}{L}\right). \quad \text{(stable)} \tag{2}$$

We may obtain from this a stability-corrected timescale.

A single molecule of H_2O is a passive tracer, because buoyancy is a body force, and does not act on a single molecule. However, a volume of moist air weighs less than an equal volume of dry air at the same temperature, so strictly there is not dynamical similarity between transport of water vapour and of a truly passive tracer (such as marked fluid elements). We have therefore chosen to express τ_L as

$$\tau_L(z) = az\left(1 - b\frac{z}{L}\right)^n/\sigma_w(z) \quad \text{(unstable)}$$

$$\tau_L(z) = az\left(1 + c\frac{z}{L}\right)^{-1}/\sigma_w \quad \text{(stable)} \tag{3}$$

and have determined a, b, c, and n by comparing predictions of the trajectory-simulation method, Equations (1), with the Project Prairie Grass (PPG) data.

The PPG data cover a very wide range of stability conditions, from a stable extreme of $L = +4.1$ m through neutral conditions ($L = \infty$) to an unstable extreme of $L = -3.2$ m. Large changes in concentration were observed as the stability changed and this enabled determination of a, b, c, and n. This is a very direct approach to the problem of the effect of stability on mass transport. In contrast, the constants 16, $\frac{1}{2}$, 5.2 in Equations (2) are in effect deduced by matching changes in concentration gradients to the stability.

2. Comparison of Trajectory-Simulation Method with the Project Prairie Grass SO_2 Diffusion Data

The Project Prairie Grass (PPG) experiments are fully described in the reports by Barad (1958) and Haugen (1959). A continuous point source of sulphur dioxide, SO_2, at a height of 46 cm above an extensive flat plain subjected a very large number of downwind detectors to a (time varying) concentration of SO_2. In each run the time average concentration was measured over a period of 10 min. All data considered herein are from the arc of detectors with radius 100 m; this was the only arc at which the vertical concentration profile was measured. Equivalent two-dimensional concentration profiles, $c(z)$, were derived by performing a crosswind integration on the concentration at $z = 150$ cm, and deducing the concentration at other heights using the profile shape measured on the (several) tall vertical masts; the shape was defined by averaging the concentration at each height over all towers which had a significant exposure and taking ratios of the values thus obtained. Care was taken to include only experiments in which the vertical profile data appeared (subjectively) reasonable. The concentration profiles $c(z)$ thus obtained should satisfy the requirement of mass conservation, that

$$\int_0^\infty c(z)u(z)\,\mathrm{d}z \leq Q$$

where Q is the source strength, $g(SO_2)\ s^{-1}$, and the inequality allows for the possibility of uptake by the (grass) surface. In agreement with Barad and Haugen, it was found that our estimates of the total horizontal flux often exceeded Q, though only by a small amount ($\leq 5\%$). We therefore treated the surface as a reflector when calculating fluid element trajectories.

For each unstable PPG run, the values of u_* and L were estimated from the windspeed and temperature profiles, assuming that the gradient Richardson number

$$\mathrm{R}_i = \frac{(g/T_0)(\partial T/\partial z)}{\left(\dfrac{\partial u}{\partial z}\right)^2} = \frac{z}{L}.$$

The second equality follows by writing $\phi_h = \phi_m^2$ where ϕ_h and ϕ_m are the universal functions for heat and momentum defined similarly to ϕ_w. Using the values of u_*, L and assuming $\phi_m = (1 - 16z/L)^{-1/4}$, a stability-corrected wind profile was defined and used in the simulation; a good fit to the observed windspeeds was always obtained.

For the stable cases, values of u_*, L were defined by assuming a log-linear wind profile

$$u = \frac{u_*}{k}\left[\ln\frac{z}{z_0} + 4.7\frac{z - z_0}{L}\right]$$

with $z_0 = 0.5$ cm, and obtaining a pair of equations for u_*, L by using the observed windspeed at 16 m and at the lowest height at which $u > 100$ cm s^{-1} (during the stable runs windspeeds near ground were in some cases low enough that one must suspect the anemometers were intermittently stalled). Therefore a good fit to the observed wind profile was always obtained. The values of u_*, L derived for each of the PPG runs analysed are given in Table I.

As was shown in I, the prediction of the trajectory-simulation method for the normalised concentration $c(z)\ u_*/Q$ due to a continuous source of strength Q in the neutral surface layer is independent of u_* (for fixed z_0 and experimental geometry).

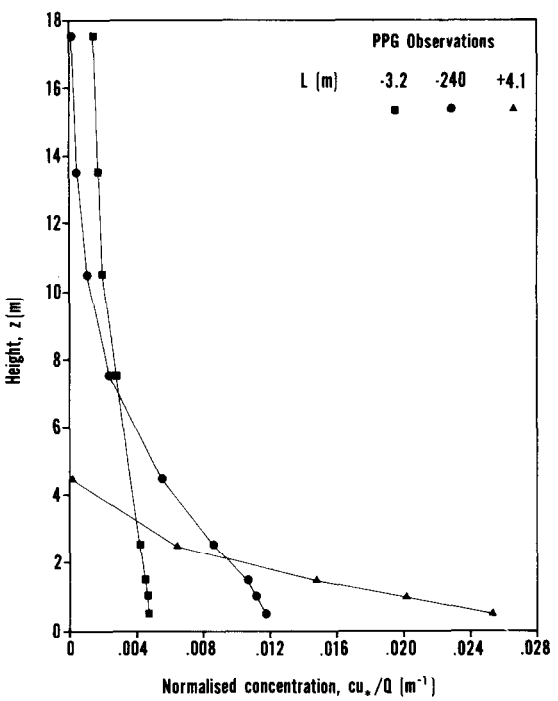

Fig. 1. Project Prairie Grass observations of normalised crosswind integrated concentration 100 m downwind of a continuous point source of SO_2 at a height of 46 cm. From left to right in symbol table, Runs 16, 57, and 14 demonstrate the very strong dependence of the normalised concentration on the Monin–Obukhov length.

In the case of the stratified surface layer, the prediction is that $c(z)\,u_*/Q$ is a function only of L (again for fixed z_0 and experimental geometry). Figure 1 shows the Project Prairie Grass measured profiles of $c(z)u_*/Q$ for a near-neutral run, an extremely unstable run, and an extremely stable run. This demonstrates the large effect of atmospheric stratification on the concentration profile at this fetch (100 m). It is worth noting that there is no constraint on the value of

$$\int_0^\infty \frac{c(z)u_*}{Q}\,\mathrm{d}z.$$

It was found that, as expected, the PPG data normalised in this manner formed a set of profiles which were well correlated with L, as is shown in Table I, which gives the values of c (50 cm) u_*/Q versus L for all the PPG runs analysed.

TABLE I

Values of u_*, L derived for the Project Prairie Grass data, and dependence of the normalised crosswind integrated concentration at z = 150 cm on the Monin–Obukhov length, L

L(m)	$\frac{c(50\text{ cm})u_*}{Q}$ (m^{-1})	u_* ($\mathrm{cm\,s}^{-1}$)	Run
− 3.2	0.0047	24	16
− 6.5	0.0060	21	25
− 7.8	0.0082	22	15
− 17	0.0103	38	43
− 26	0.0107	44	50
− 28	0.0085	36	19
− 32	0.0105	41	44
− 36	0.0114	45	49
− 37	0.0114	34	62
− 38	0.0111	42	26
− 39	—	48	61
− 45	0.0119	46	30
− 62	0.0115	62	20
− 93	0.0122	55	33
−110	0.0147	41	45
−240	0.0117	50	57
+ 13.4	0.0171	19	18
+ 7.3	0.0240	13.6	59
+ 6.0	0.0205	9.0	36
+ 4.7	0.0250	10.2	32
+ 4.1	0.0253	6.8	14

The profiles in Figure 1 (i.e., the extreme cases) were used to choose a, b, c, and n; the resulting choices for the stability-corrected timescale were then used to perform simulations of intermediate cases.

2.1. NEAR-NEUTRAL CONDITIONS

Run 57, with $L = -240$ m, was chosen in order to determine the constant 'a' in Equations (3). The estimated total horizontal flux was 92 gs^{-1}, and the quoted source strength 102 gs^{-1}. Barad notes that there may have been a technical failure during this run. Had this occurred before the run started, the samplers at 150 cm would have collected no SO_2. The close agreement between estimated horizontal flux and source strength suggests that there was no technical failure, or, at worst, it was late in the run.

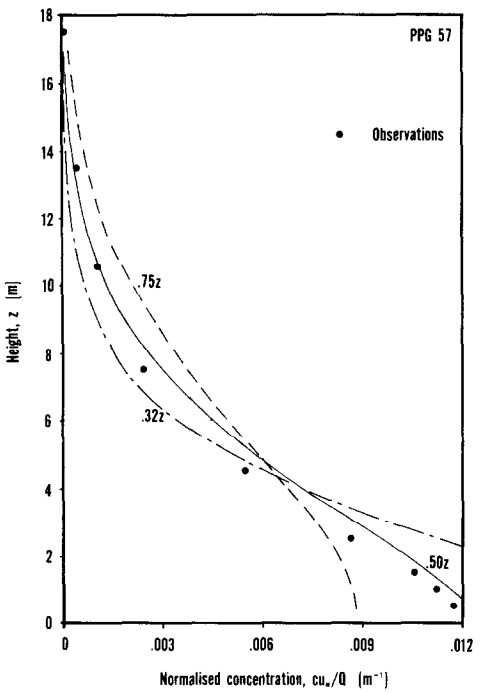

Fig. 2. Predictions of the trajectory-simulation method for PPG run 57 ($L = -240$m) using $\Lambda_L/z = 0.32$, 0.50 and 0.75.

Figure 2 shows the observed concentration and predictions using Equations (1 and 3) with $b = 0$, $\sigma_w = 1.25u_*$ and $a = (0.32, 0.5, \text{and } 0.75)$. The choice $\Lambda_L = 0.32z$ corresponds to the widely accepted estimate of the length scale for momentum transport under neutral conditions; if

$$\sigma_w \simeq 1.25u_*,$$

then

$$K_m = 0.4u_*z \simeq 0.4\frac{\sigma_w}{1.25}z = 0.32\sigma_w z.$$

The length scale assumed for mass transport in neutral stratification must exceed

$0.32z$ in order that the concentration profile determined by the trajectory-simulation method should compare closely with the observations. With $a = 0.5$, we predict a profile $u_* c(z)/Q$ which is extremely close to that observed (a little larger, as is required by continuity, when the surface is a reflector). A value of 0.5 for 'a' was also found by Reid (1979) by comparison of a similar trajectory-simulation method with the Porton experiments. In all other simulations we therefore kept $a = 0.5$.

2.2. Very unstable stratification

Run 16 was in the most unstable conditions, with $L = -3.2$ m. For $z \gtrsim 6$ m, $|z/L|$ is beyond values encountered in deriving the stability dependence of ϕ_m, ϕ_h, ϕ_w. In such unstable conditions, one would expect σ_w to change with height above $z \simeq 0.5|L| = 160$ cm; variation of σ_w implies the need for a bias added to the particle velocity in the z_* system

$$\begin{aligned}\bar{w}_{*L} &= \sigma_w(H)\tau_L(z)\frac{\partial \sigma_w}{\partial z} \\ &= \sigma_w(H)\Lambda_L(z)1/\sigma_w \frac{\partial \sigma_w}{\partial z} \\ &= \sigma_w(H)\Lambda_L(z)\left(\tfrac{1}{3}\right)\left(\frac{4.1}{-L}\right)\Big/\left(1 + 4.1\frac{z}{-L}\right).\end{aligned}$$

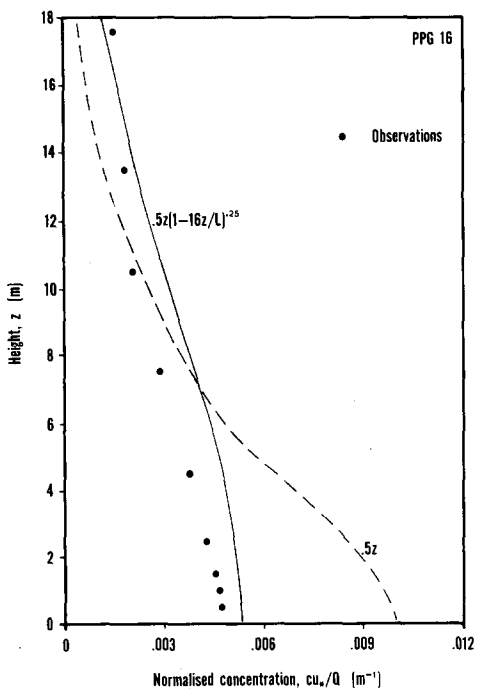

Fig. 3. Predictions of the trajectory-simulation method for PPG run 16 ($L = -3.2$ m) with no stability correction to the length scale and with a correction factor of $(1 - 16z/L)^{1/4}$.

We would expect the predicted trajectories to be inaccurate at any z such that

$$\Lambda_L(z) \not< |S| = \left|\frac{\partial\sigma_w/\partial z}{\partial^2\sigma_w/\partial z^2}\right| = \tfrac{3}{2}\left(\frac{-L}{4.1}\right)\left(1 - 4.1\frac{z}{L}\right). \tag{4}$$

Figure 3 shows the observed concentration and predictions with $\sigma_w = 40$ cm s^{-1} for all z (the value observed at $z = 200$ cm) and

(i) No stability correction to the length scale (but with stability-corrected wind profile).

(ii) $\Lambda_L = 0.5z\,(1 - 16z/L)^{1/4}$.

Clearly a stability correction is necessary. It was found that use of $\Lambda_L = 0.5z$ $(1 - 16(z/L))^{1/2}$, which follows from the Dyer and Hicks stability correction for water vapour if the height-dependence of σ_w is ignored, gave an excessively large correction.

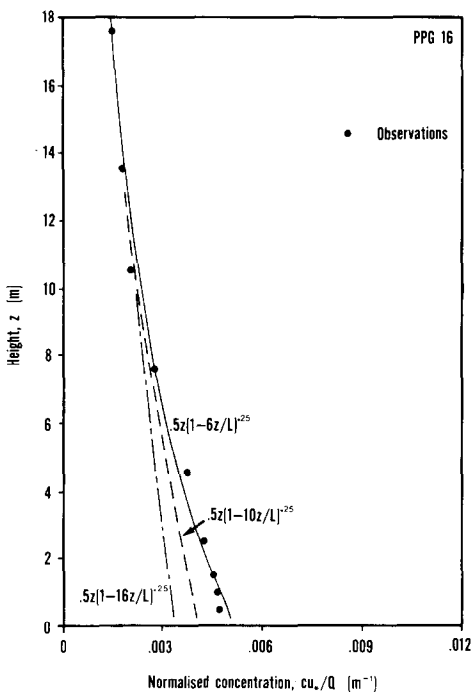

Fig. 4. Predictions of the trajectory-simulation method for PPG run 16 ($L = -3.2$ m) with three choices of the stability correction to the length scale. In all cases a bias velocity $\bar{w}_{*_L}$ has been added to the turbulent velocity in the z_* system to incorporate the effect of height-dependence of σ_w.

Figure 4 again shows the observed data, and predictions with $\sigma_w = 26$ $(1 - 4.1z/L)^{1/3}$, which gives $\sigma_w(200) = 40$ cm s^{-1}, and

(i) $$\Lambda_L = 0.5z\left(1 - 16\frac{z}{L}\right)^{1/4}$$

(ii) $$\Lambda_L = 0.5z\left(1 - 10\frac{z}{L}\right)^{1/4}$$

(iii) $$\Lambda_L = 0.5z\left(1 - 6\frac{z}{L}\right)^{1/4}.$$

In all cases a bias velocity $\bar{w}_{*L}$ has been applied in calculating the particle trajectories. This allowance for the gradient in σ_w alters the predicted profile shape considerably. Predicted concentration is fairly insensitive to large changes in b. For the choice $b = 6$, there is good agreement between predicted and observed concentration. Investigating the constraint, Equation (4), it is found that with this choice for Λ_L, and $L = -3.2$ m,

$$\Lambda_L < |S| \quad \text{for} \quad z < 45 \text{ m}.$$

Therefore the application of the bias velocity in order to allow for the gradient in σ_w is valid (for distances of short enough travel that only a small number of particles exceed a height of $\simeq 45$ m).

2.3. Intermediate unstable cases

Figure 5 compares the prediction of the trajectory-simulation method using $\Lambda_L = 0.5z\,(1 - 6z/L)^{1/4}$ with the observations of runs 15 and 50 ($L = -7.8, -26$ m).

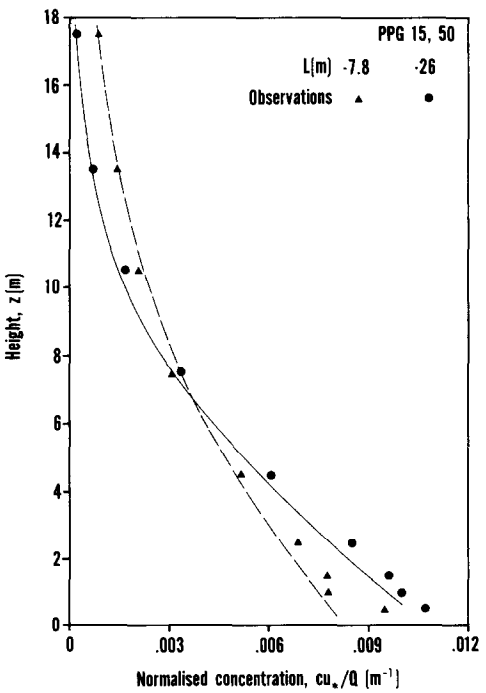

Fig. 5. Predictions of the trajectory-simulation method for PPG runs 15, 50 ($L = -7.8$ m, dashed curve; $L = -26$ m, solid curve) using $\Lambda_L(z) = 0.5z(1 - 6z/L)^{1/4}$.

Although the above stability correction for Λ_L has given a slight underestimate of concentration below ~ 4 m, the percentage error is small at all heights.

2.4. Very stable stratification

Run 14 was performed under very stable stratification, with the estimate of L being $+4.1$ m. Figure 6 shows the observations and the results of simulations performed using $\Lambda_L = 0.5z/(1 + cz/L)$ with $c = 2, 5, 10$. The best choice is $c = 5$.

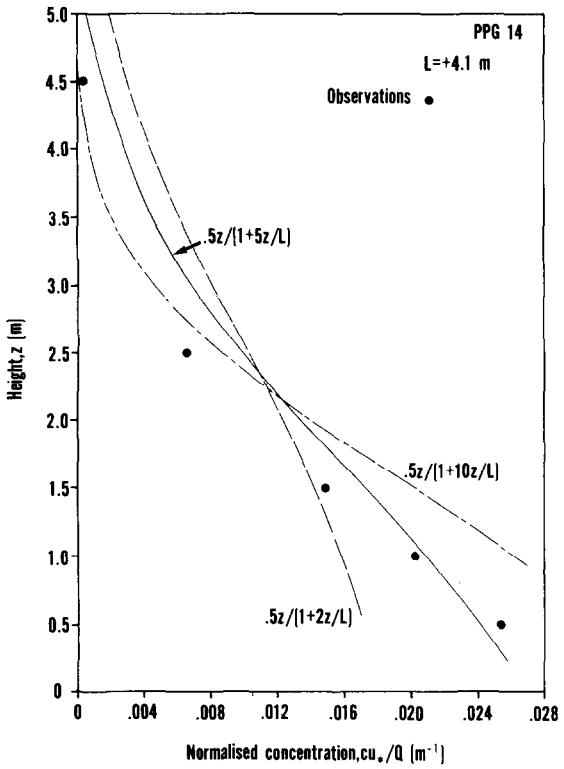

Fig. 6. Predictions of the trajectory-simulation method for PPG run 14 ($L = +4.1$ m) for three choices of the Lagrangian length scale.

2.5. Intermediate stable case

Figure 7 demonstrates excellent agreement between the prediction of the trajectory-simulation method using $\Lambda_L = 0.5z/(1 + 5z/L)$ and the observations of run 59 ($L = +7.3$ m).

3. Comparison of Trajectory-Simulation Method with Glass Bead Tracer Experiments

In order to provide an independent test of Equations (1), experiments were performed using highly spherical glass beads of uniform size (40 μm diameter) as a tracer in the turbulent motion above an immature crop of corn (similar experiments within a mature crop will be described elsewhere).

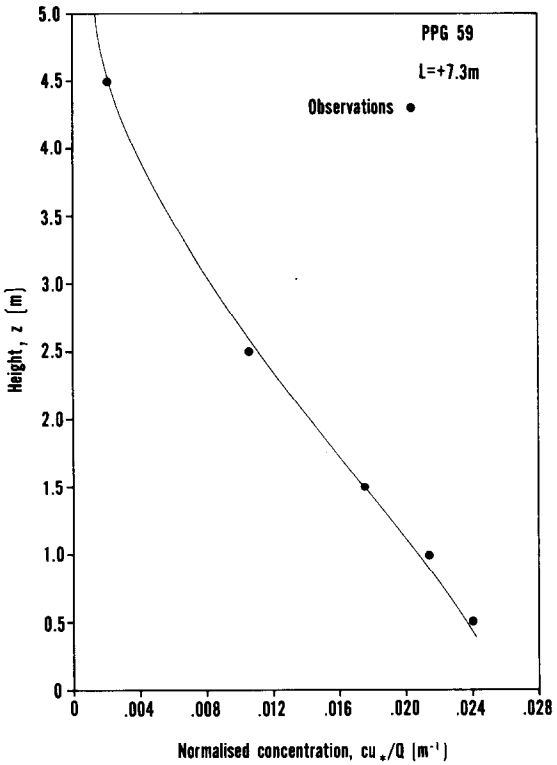

Fig. 7. Prediction of the trajectory-simulation method for PPG run 59 ($L = +7.3$ m) using $\Lambda_L = 0.5z/(1 + 5z/L)$.

The beads were obtained from the Cataphote Corporation*, who classified them as 'close sized uni-spheres, 95% true spheres, 95% in range (−325 + 400 mesh), density 2.42 g cm^{-3}'. On examination of 1000 randomly chosen beads, it was found that 95% had diameters between 35 and 45 μm; from the size distribution, a frequency-weighted settling velocity of 12 cm s^{-1} was deduced, using Stoke's law. Concentration of the beads in the air was measured using glue-coated plastic rods of 1.5 × 1.5 mm cross-section mounted on voltage-insensitive constant rpm motors** ($\simeq$ 2400 rpm, individually calibrated using a strobescope) mounted on portable masts. The collection efficiency, ε, should lie between 0.7 and 1.0, given the size and density of the beads. Care was taken to ensure that all collection rods were coated and dried identically.

The beads were counted on the rods at a magnification of × 10. Very few ($\ll 5\%$) beads were found to be paired together, indicating good dispersal by the source. Any very heavy clumps of beads would not have been captured. However observation of the plume at the source revealed no such clumps.

* 1750 Sismet Rd., Mississauga, Ontario, Canada.

** Ted Brown Associates, 26338 Esperanza Drive, Los Altos Hills, California, 94022, U.S.A.

If several collectors are placed in a cloud of beads of uniform density, and if on unit area of each collector we observe $n_1, n_2 \ldots n_N$ beads, then these estimates will be distributed about the 'true' count n with variance $\sigma^2 = n$. Therefore the larger the n_i, the smaller the spread as a proportion of n. In order to obtain good statistical reliability, experiments were run for a time long enough to ensure a count $\gtrsim 500$ on all rods (usually a time of $\simeq 2$ h for a source-collector distance $\simeq 30$ m) but not so long as to result in a large proportion of the area of the collectors being covered in beads (so as to avoid a decrease in collection efficiency).

In two preliminary trials, 8 collectors were placed together at $z = 1$ m, a distance of 25 m downwind of the source, which was at $z = 2$ m. The results were

(i) 1 h exposure

Average of 8 values of the count on 9 mm^2 = 76 beads.
Implied sample standard deviation $\sqrt{76} = 8.7$.
Observed standard deviation = 6.3.

(ii) 2 h exposure

Average of 8 values of the count on 19 mm^2 = 386 beads.
Implied sample standard deviation $\sqrt{386} = 19.6$.
Observed standard deviation = 20.

The site of the diffusion experiments was a large field at the Elora Research Station, Elora, Ontario, Canada. The upstream extent of uniform surface conditions was $\simeq 400$ m. Windspeeds were measured using miniature cup anemometers (stopping speed < 50 cm s^{-1}) which were calibrated in a wind tunnel prior to the field season against a pitot tube using a sensitive capacitive pressure transducer. A single-axis sonic anemometer*, also calibrated against the pitot tube, was used to measure σ_w at a height of 250 cm during the experiments – the output of this anemometer was sampled at 100 Hz by a Honeywell 316 minicomputer.

Twelve detectors were used, four on each of three masts. The masts were placed on an arc centred on the source and of chosen radius, at such a position as to give a traverse across the plume centre-line. Experiments were performed in rather windy conditions, when the plume direction was fairly steady. If the wind direction did change, the mast farthest from the plume was moved around the arc back into the plume. The intention was to get a good estimate of the vertical profile shape (except in the experiment of 2 November 1979), so the lateral positions of the masts were not recorded. Because a lateral sample at only 3 points was considered insufficient to obtain an accurate cross-wind integrated absolute concentration, the rate of bead release was not measured (but should have been close to the value measured on 2 November 1979, 1.49×10^6 beads s^{-1}).

The 'Stokesian response time' (time constant for response of bead velocity to a step change in the velocity of the fluid surrounding it) of the beads was $\tau_p = 0.012$ s. Therefore in all simulations the beads were given a steady settling velocity $\bar{w}_g$ (added

* Campbell Scientific Inc., P.O. Box 551, Logan, Utah 84321, U.S.A.

to their turbulent velocity) because except near the surface $\tau_p \ll \tau_L(z)$ and therefore the bead can be regarded as instantaneously taking on a velocity

$$w^{\text{turbulent}} - \bar{w}_g.$$

The surface was treated as a perfect sink at $z = z_0$.

3.1. Detailed measurement of the lateral concentration profile for determination of the absolute equivalent two-dimensional concentration

On 2 November 1979 an experiment was run with all 12 detectors at $z = 54$ cm above a bare field in an arc of radius 20 m, centred on the source which was at $z = 235$ cm. Over 30 min, 220 g of beads were released at a constant rate of 0.122 g s^{-1}, which corresponds to a rate of release of 1.49×10^6 (beads s^{-1}). Figure 8 shows

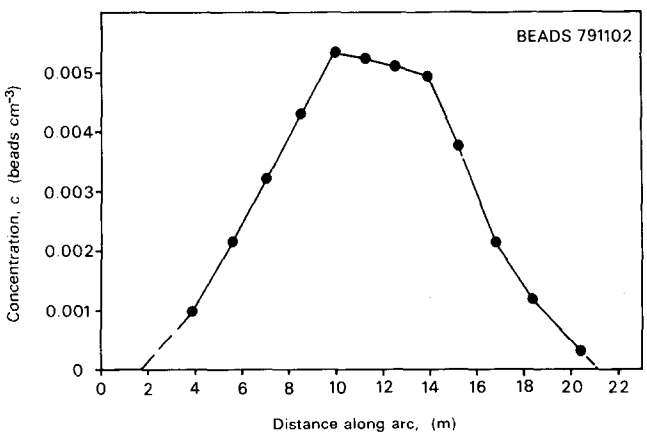

Fig. 8. Lateral concentration profile at $z = 54$ cm around an arc of radius 20 m centered on a continuous point source of glass beads at $z = 235$ cm. Duration of experiment 30 min.

the measured crosswind profile of average bead concentration (the highest concentration corresponds to a count of 101 beads per 1 mm^2 on the collecting rod). Note that a collection efficiency (ε) of 1 has been assumed. A crosswind integration yields a value for the equivalent average two-dimensional concentration at $z = 54$ cm of 5.5 beads cm^{-2}. This should be interpreted as follows: if all the beads remained on a vertical plane (no crosswind), then 5.50 beads would lie in each 1 cm^2 area at a distance of 20 m from the source and a height of 54 cm.

The observed wind profile is given in Table III, and is well fitted by $u(z) = (45/0.4) \ln(z/1.45)$, whence $u_* = 45$ cm s^{-1}. The sonic anemometer measured $\sigma_w = 63$ cm s^{-1} ($\sigma_w/u_* = 1.40$).

Equations (1) were used to simulate this experiment, without any stability correction because the wind was moderate, the beads confined very close to ground over the distance of travel, and the soil very wet. We used

$\bar{w}_g = 12$ cm s^{-1}, $\sigma_w = 63$ cm s^{-1}, and

(i) $\Lambda_L = 0.32z$, (ii) $\Lambda_L = 0.50z$.

The corresponding predictions for the absolute two-dimensional concentration at $z = 54$ cm were

(i) $c(54) = 4.9$ beads cm^{-2}, implying $\varepsilon = 1.12$

(ii) $c(54) = 5.5$ beads cm^{-2}, implying $\varepsilon = 1.0$.

Note that if $\Lambda_L/z < 0.5$, we would require $\varepsilon > 1$ to match the experimental measurement.

3.2. Profile Experiments

Tables II and III give the experimental geometry and meteorological data for 3 experiments over an immature corn canopy. The observed bead counts are given in Table IV (and may be converted to concentration, noting that the volume swept

TABLE II

Experimental details of glass-bead diffusion trials over an immature corn canopy

Date	July 1, 1979	July 2, 1979	July 16, 1979
Source Height (cm)	251	251	80
Radius (fetch), (cm)	3650	2000	1540
Duration (min)	165	60	300
Corn Height (cm)	20	20	$\simeq 70$
Comments	heavily overcast strong wind damp soil	1/10 Cu light wind damp soil	2/10 Cu dry soil
Sonic σ_w (cm s^{-1})	70	50	—
Fit to observed wind profile $u(z)$, cm s^{-1}	$\frac{59}{0.4}\ln\frac{z}{2.45}$	$\frac{40}{0.4}\ln\frac{z}{1.6}$	$\frac{57}{0.4}\ln\frac{z-20}{12.4}$
σ_w/u_*	1.19	1.25	— (used 1.25)

TABLE III

Wind profiles (cm s^{-1}) for the glass-bead diffusion trials

Height (cm)	July 1, 1979	July 2, 1979	July 16, 1979	Nov. 2, 1979
54	455 cm s^{-1}	343	142	424
108	556	422	283	460
188	625	471	367	528
287	699	516	439	577
423	758	547	495	606

TABLE IV

Bead count on 40 mm^2 of collector surface, normalised to 2400 rpm

Height	Day of experiment (July 1979)	Mast A	Mast B	Mast C
	01	4316	2618	4995
40	02	596	573	1123
	16	—	—	—
	01	4318	2744	4911
90	02	833	884	1440
	16	6178	3373	8800
	01	4539	2715	4478
150	02	1007	978	1549
	16	7705	4468	8616
	01	4016	2411	—
220	02	908	789	—
	16	6125	3450	7534
	01	—	—	—
310	02	—	—	—
	16	3835	2228	4859

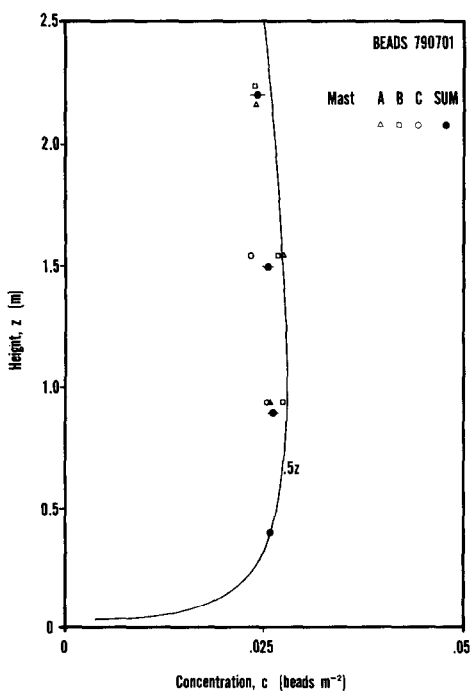

Fig. 9. Prediction of the trajectory-simulation method and observed bead concentration profile (matched at z = 40 cm) for experiment of July 1, 1979. Source height 251 cm, fetch 3650 cm.

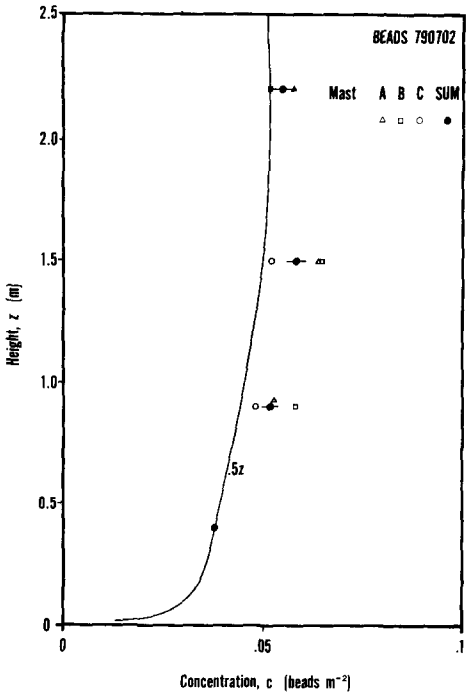

Fig. 10. Prediction of the trajectory-simulation method and observed bead concentration profile (matched at $z = 40$ cm) for experiment of July 2, 1979. Source height 251 cm, fetch 2000 cm.

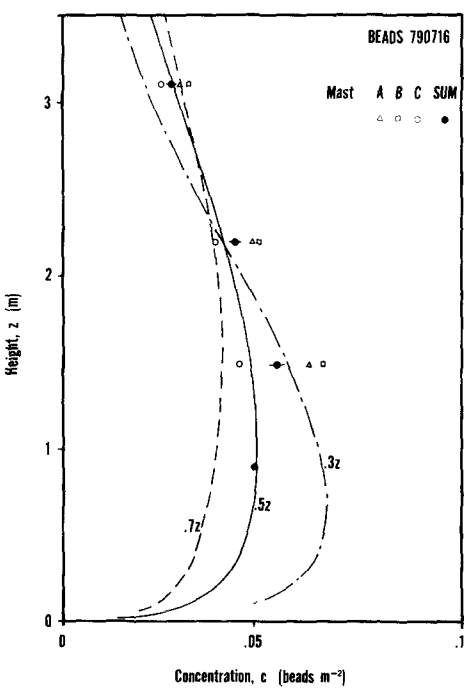

Fig. 11. Predictions of the trajectory-simulation method with $\Lambda_L/z = 0.3$, 0.5, 0.7 and observed bead concentration profile (matched at $z = 90$ cm to the prediction with $\Lambda_L = 0.5\ z$) for experiment of July 2, 1979. Source height 80 cm, fetch 1540 cm.

out in 1 revolution by 1 mm^2 of detector area is 269 mm^3). In Figures 9, 10, and 11 the observed profile shapes have been compared with those predicted by the simulation technique, using a source strength of 1 bead s^{-1}, by forcing the observations to fit at the lowest measurement height. The error bars give the range within which 66% of all repetitions of the experiment would place the data point, assuming errors to be purely random.

In each case the experiment has been simulated using $\Lambda_L = 0.5\ z$. For the experiment of July 16, 1979, simulations were also performed with $\Lambda_L = (0.3, 0.7)z$; these are also plotted to demonstrate that $\Lambda_L/z = 0.5$ gives best agreement. The vertical profile shape on a single mast and the average (over 3 masts) profile shape give only an approximate estimate of the vertical profile of crosswind integrated concentration, which is the profile predicted by the model. This is probably the reason for the small differences between observed and predicted profile shapes.

4. Conclusion

Two previous papers showed that the trajectory-simulation method agrees with analytical solutions for the concentration downwind of continuous sources in homogeneous turbulence and in turbulence with power law wind and diffusivity profiles. This paper has demonstrated that if the Lagrangian length scale is chosen as

$$\Lambda_L = 0.5\, z \left(1 - 6\frac{z}{L}\right)^{1/4} \qquad L < 0$$

$$\Lambda_L = 0.5\, z \Big/ \left(1 + 5\frac{z}{L}\right) \qquad L > 0$$

one may simulate trajectories in the atmospheric surface layer to obtain accurate estimates of short-range turbulent dispersion over a wide range of values of the Monin–Obukhov length (-3.2 m through ∞ to $+4.1$ m). It is therefore felt that the trajectory-simulation method may be applied with confidence to many problems of practical interest which cannot be easily or satisfactorily solved by Eulerian methods.

Although the majority of this work has been done using an assembly language program (on a Honeywell H316 minicomputer), a Fortran version is now in use. It is stressed that the program required to simulate a trajectory is very simple.

Limitations of the method should be discussed. Firstly, in the case where σ_w is height-dependent, one must bias trajectories in the direction of increasing σ_w. At present, it is not known how this may be correctly achieved for an arbitrary profile of σ_w. The method used herein, addition of a bias velocity $\bar{w}_L = \Lambda_L \partial\sigma_w/\partial z$, is believed to be valid for the unstable surface layer. Further attention must be given to the implications of a gradient in σ_w before the method can be applied to diffusion in agricultural or forest canopies.

Secondly, although it is hoped that eventually it will be possible to simulate trajectories correctly over very long distances, the work described herein is limited

to diffusion problems in which the majority of the trajectories are confined to the layer in which the chosen profiles of u, σ_w, and Λ_L are valid.

Thirdly, in all work presented to date, the surface has been treated either as a perfect reflector or a perfect sink at z_0. In many important problems (e.g., SO_2 diffusion over wet grass) the surface is an imperfect sink (often characterized by a surface uptake resistance); this situation may be dealt with by partial reflection at z_0.

Finally, the question of generalization to three-dimensional flow and to inhomogeneous terrain arises. Addition of a fluctuating crosswind component (with scale σ_v) is in principle straightforward. However, the dominant eddies contributing to σ_v have periods much longer than those dominating σ_w (see Haugen, 1973) so that a three-dimensional trajectory-simulation could only be applied to an experiment during which the turbulence is stationary over a period considerably longer than the 10 min employed in the Project Prairie Grass experiments (in which the vertical profile shapes were very smooth, but the horizontal profile shapes, in many cases, quite irregular). In addition to this, it is not possible to predict σ_v given u_* as accurately as is the case with σ_w (σ_v does not follow Monin–Obukhov similarity).

The difficulties which arise when σ_w is height-dependent imply that it is not necessarily an easy matter to simulate fluid element movement correctly over inhomogeneous terrain, even given descriptions of the mean and turbulent flow patterns.

In spite of the limitations discussed above, there remain many problems which may now be usefully investigated using the trajectory-simulation method.

References

Abramowitz, M., and Stegun, I. A.: 1970, *Handbook of Mathematical Functions*, Dover Publications Inc., New York.

Barad, M. L.: 1958, 'Project Prairie Grass, a Field Program in Diffusion (Vol. II)', Geophysical Research Papers No. 59, Air Force Cambridge Research Centre – TR-58-235(II).

Businger, J. A., Wyngaard, J. C., Izumi, Y., and Bradley, E. F.: 1971, 'Flux-profile Relationships in the Atmospheric Surface Layer', *J. Atmos. Sci.* **28**, 181–189.

Dyer, A. J. and Hicks, B. B.: 1970, 'Flux-Gradient Relationships in the Constant Flux Layer', *Quart. J. Roy. Meteorol. Soc.* **96**, 715–721.

Haugen, D. A.: 1959, 'Project Prairie Grass, a Field Program in Diffusion (Vol. III)', Geophysical Research Papers No. 59, Air Force Cambridge Research Centre – TR-58-235(III).

Haugen, D. A.: 1973, *Workshop on Micrometeorology*, Publication of the American Meteorological Society, Boston, Massachusetts.

Reid, J. D.: 1979, 'Markov Chain Simulations of Vertical Dispersion in the Neutral Surface Layer for Surface and Elevated Releases', *Boundary-Layer Meteorol.* **16**, 3–22.

Ward, D. P.: 1977, 'Some Observations of Atmospheric Turbulence Within and Above a Corn Canopy using a Modified Split Film Heat Transfer Anemometer', M.Sc. thesis, University of Guelph, Guelph, Ontario, Canada.

Webb, E. K.: 1970, 'Profile Relationships: The Log-Linear Range, and Extension to Strong Stability', *Quart. J. Roy. Meteorol. Soc.* **96**, 67–90.

Wilson, J. D., Thurtell, G. W., and Kidd, G. E.: 1981a, 'Numerical Simulation of Particle Trajectories in Inhomogeneous Turbulence, I.: Systems with Constant Turbulent Velocity Scale', *Boundary-Layer Meteorol.* **21**, 295.

Wilson, J. D., Thurtell, G. W., and Kidd, G. E.: 1981b, 'Numerical Simulation of Particle Trajectories in Inhomogeneous Turbulence, II: Systems with Variable Turbulent Velocity Scale', *Boundary-Layer Meteorol.* **21**, 423.